

Spin blockade in capacitively coupled quantum dots

M. C. Rogge, C. Fühner, U. F. Keyser, and R. J. Haug

Citation: *Appl. Phys. Lett.* **85**, 606 (2004); doi: 10.1063/1.1776613

View online: <https://doi.org/10.1063/1.1776613>

View Table of Contents: <http://aip.scitation.org/toc/apl/85/4>

Published by the [American Institute of Physics](#)



2. YOUR AC IS LEAKING
The main reason for the observed...
VOLTAGE SOURCE EXAMPLE
CURRENT SOURCE EXAMPLE

5. COAXIAL
These diagrams show the...
COAXIAL
TWO-WIRE

5 Electronic Measurement Pitfalls to Avoid

Get the whitepaper

Spin blockade in capacitively coupled quantum dots

M. C. Rogge,^{a)} C. Fühner, U. F. Keyser, and R. J. Haug

Institut für Festkörperphysik, Universität Hannover, Appelstrasse 2, 30167 Hannover, Germany

(Received 24 October 2003; accepted 3 June 2004)

We present transport measurements on a lateral double dot produced by combining local anodic oxidation and electron beam lithography. We investigate the tunability of our device and demonstrate that we can switch on and off tunnel coupling between both dots in addition to capacitive coupling. In the regime of pure capacitive coupling, we observe the phenomenon of spin blockade in a magnetic field and analyze the influence of capacitive interdot coupling on this effect. © 2004 American Institute of Physics. [DOI: 10.1063/1.1776613]

In recent decades great progress has been made in the development and measurement of quantum dot devices.¹ Many single electron transistors have been fabricated and during the last several years coupled quantum dots (e.g., Refs. 2–6) have come more and more into the focus of research, as they are proposed as crucial parts for quantum computers.⁷ Since preparation and detection of electron spin is another essential element in future quantum information applications, the discovery of several spin blockade mechanisms in quantum dot devices was a great step forward. Blocked transport can occur due to spin selection rules in single quantum dots.⁸ Another spin selective mechanism based on Pauli exclusion blocks the interdot transport in a coupled dot system.⁹ In this letter we refer to a third mechanism that was introduced by Ciorga *et al.*^{10–12} It is explained by spin polarized leads and has been observed in single quantum dots defined by metallic gates. Coupled quantum dots are also of great interest in the regime of this spin blockade where recently spin resolved measurements on molecular states of two dots tunnel coupled in series have been made.¹³

In this letter we present our results for spin blockade in a parallel double quantum dot based on local anodic oxidation (LAO). Due to the complexity of the device we first have to characterize our system in terms of the interdot coupling, which depends on top gate voltage and magnetic field. We find that the relevant regime, where we observe spin blockade, features capacitive coupling only. We show our measurements for spin blockade and analyze the influence of capacitive interdot coupling on this effect.

Our quantum dot device is based on a GaAs/AlGaAs heterostructure with a two-dimensional electron system (2DES) 34 nm below the surface. The sheet density is $n = 4.3 \times 10^{15} \text{ m}^{-2}$. We apply two different nanolithographic techniques to the sample surface to define two adjacent quantum dots connected in parallel to common source and drain contacts. We use an atomic force microscope (AFM) to write the basic double dot structure by local anodic oxidation. We complete the structure with a metallic gate patterned with electron beam lithography (e-beam) to add the function of controlled tunability of the interdot coupling.

An AFM image of our device is given in Fig. 1(a). Parts that have been fabricated by LAO are colored blue. They represent insulating lines, which form a complete double dot device including the two dots A and B, side gates G1 and G2

and source (S) and drain (D) leads. The two dots are connected via 80- to 100-nm-wide tunneling barriers to the leads and via a central barrier to each other. An additional metallic top gate (golden) can be biased to tune the height of the central barrier and thus to tune the interdot coupling. A detailed description of a similar device and the fabrication technique can be found in Ref. 14.

Our double dot device is characterized in transport measurements in a ³He/⁴He dilution refrigerator at a base temperature of 70 mK. We apply standard lock-in technique to measure the differential conductance G through the double dot system. From the total capacitances and the geometrical shapes we can roughly estimate electron numbers of 120 for dot A and 240 for dot B. To analyze the features for spin blockade, which will be shown later, it is first necessary to understand the interaction of both dots in the relevant parameter space. Therefore we start investigating the interdot coupling with the top gate grounded at $B=0$ T. Figure 1(b) shows G under these conditions as a function of both side gate voltages V_{G1} and V_{G2} . The dark regions denote high values for G and represent transport over dot A. No lines corresponding to transport over dot B are visible meaning that B is not connected to both leads. Nevertheless the equidistant splittings interrupting the features of dot A indicate the presence of dot B, which is connected to the source lead while the drain lead remains closed for all the parameters used here, as we know from nonlinear measurements (not shown here). This is due to the lithographic gap width of only 70 nm for the barrier between dot B and drain compared to 80–100 nm for the other barriers. Thus we can complete the observed features by dotted lines to a hexagonal pattern typical for two coupled quantum dots. Crossing a dark line changes the electron number on dot A (N_A), crossing a dotted line changes the charge on dot B (N_B). Due to the sharp corners of the hexagons and the fact that the only features visible are those of dot A, the interdot coupling in this regime is purely capacitive.

Figure 1(c) shows a similar plot but with the top gate voltage set to 80 mV. Due to the reduced height of the central barrier at $V_{TG}=80$ mV the interdot coupling has increased leading to a very wide splitting. In contrast to Fig. 1(b) the edges of the hexagonal pattern are clearly rounded and there are finite conductance values visible for transitions on dot B. Both effects demonstrate the molecular like character of the system. Instead of atomic transitions the visible features refer to molecular binding states indicating tunnel coupling.^{15,16}

^{a)}Electronic mail: rogge@nano.uni-hannover.de

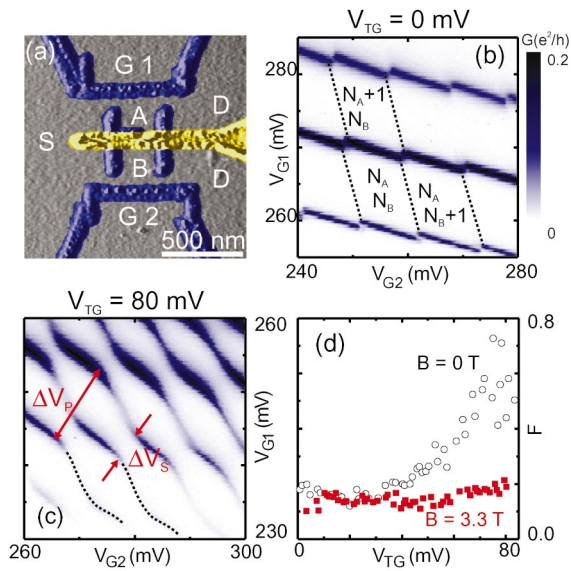


FIG. 1. (Color) (a) Colorized AFM image of our double dot device. Oxide lines (blue) define source (S) and drain (D) leads, side gates G1 and G2, and two quantum dots A and B. A metallic top gate (golden) is added by e-beam lithography. (b) G as a function of both side gate voltages V_{G1} and V_{G2} for $V_{TG}=0$ mV. The Coulomb blockade of dot A is interrupted by regular splittings referring to transitions on dot B. (c) Similar plot for $V_{TG}=80$ mV. The splitting has increased, round edges and additional features completing the hexagonal pattern represent molecular binding states. (d) Fractional peak splitting F as a function of top gate voltage V_{TG} for $B=0$ T and $B=3.3$ T.

A more detailed view can be gained by calculating the fractional peak splitting $F=2\Delta V_S/\Delta V_P$ [see Fig. 1(c)], which is 0 for two separate dots and 1 for two totally merged dots.¹⁷ Figure 1(d) shows F as a function of top gate voltage for $B=0$ T (open circles). For voltages below 30 mV the fractional peak splitting is unaffected by V_{TG} and remains at values below 0.2. This is due to capacitive coupling, that depends on the LAO geometry of both dots, which is almost not affected by top gate voltage. At 30–40 mV tunnel coupling sets in and molecular features appear. With increasing top gate voltage the fractional peak splitting can be tuned to almost 0.8 corresponding to very strong tunnel coupling.

The interdot coupling is not only changed by top gate voltage but also by a magnetic field applied perpendicular to

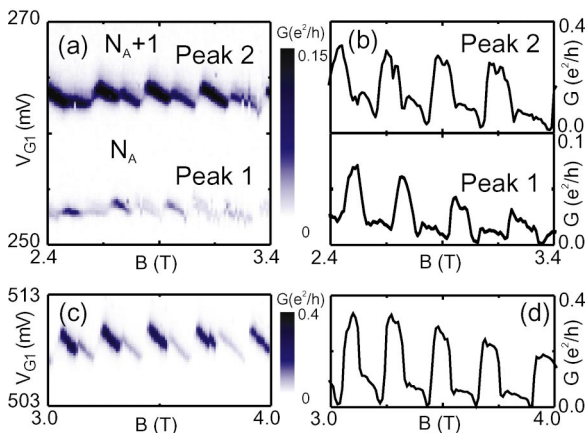


FIG. 2. (Color) (a) G as a function of V_{G1} and magnetic field for $V_{TG}=0$. The two Coulomb peaks of dot A show oscillations in peak position in the regime of spin blockade. (b) The maxima for both peaks as a function of B show a spin dependent height, high values for spin down transport, low values for spin up. (c) and (d) A similar measurement for a different cooling cycle.

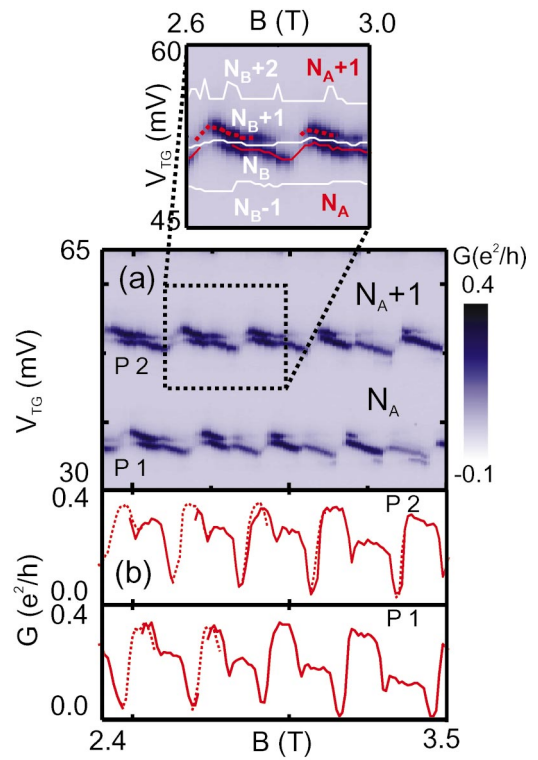


FIG. 3. (Color) (a) G as a function of V_{TG} and magnetic field. The peaks of dot A (red lines in the section) show oscillating positions. Due to capacitive coupling these peaks are regularly split by transitions on dot B (white lines). Thus each peak occurs below (solid line) and above (dotted line) such a splitting. (b) The maxima for both peaks show again an alternating height caused by single dot spin blockade. The amplitudes for parts of a peak below a splitting (solid) and for parts above a splitting (dotted) fit almost perfectly together. Thus capacitive dot–dot coupling has no effect on spin blockade.

the 2DES. At $B=3.3$ T the fractional peak splitting is again decreased to a value below 0.2 and remains unaffected by top gate voltage [squares in Fig. 1(d)]. The magnetic field destroys the tunnel coupling and moves the system back to the regime of capacitive coupling even with $V_{TG}=80$ mV.

After having characterized our double dot we can now focus on the features of spin blockade, which appear around 3.3 T in the regime of capacitive coupling.

Figure 2(a) shows G as a function of V_{G1} and B . Two Coulomb peaks are visible denoting transitions on dot A. For both peaks, oscillations in peak position are obvious as well as alternating amplitudes for the peak maxima [see Fig. 2(b)]. The amplitude is changed by magnetic field and by electron number N_A . Therefore this effect looks similar to the effect of spin blockade that has been observed in several single dot devices.^{10,11} We observed this effect in several cooling cycles. Figures 2(c) and 2(d) show a similar measurement for a different cooling cycle. We were also able to confirm the spin blockade behavior in nonlinear measurements (not shown here), which are comparable to those of Ciorga *et al.*¹² The fields of 3–4 T used here to observe spin blockade are higher than those of Ciorga *et al.* of only 0.5–1.5 T. This is probably due to the higher electron density of $4.3 \times 10^{15} \text{ m}^{-2}$ in our sample compared to $1.7 \times 10^{15} \text{ m}^{-2}$ in the sample of Ciorga *et al.*¹⁰

Spin blockade is explained as follows. As source and drain consist of a 2DES, they develop edge channels in a magnetic field. If the potential is flat enough these channels are separated in space leaving a spin down channel of the

lowest Landau level near to the dot and a spin up channel further away. Thus the overlap of electronic wave functions of leads and dot is spin dependent. Spin up electrons couple weaker to the dot than spin down electrons. Therefore transport with spin up electrons is suppressed. A magnetic field changes the available spin state for electrons tunneling into the dot,¹⁸ which becomes obvious in alternating peak positions and peak amplitudes of Coulomb blockade peaks. LAO devices are known to have steeper potentials than split gate devices.^{19,20} Thus the spatial separation of edge channels in the leads is believed to be much smaller in LAO devices. Spin blockade should be very improbable or at least suppressed in comparison to split-gate devices and has actually not been measured in LAO devices so far.

Nevertheless, despite the LAO nature we observe these features here very clearly, and although this is a coupled dot system, we assume that this observation is due to spin blockade in dot A only, since we are in the regime of capacitive coupling. Nevertheless the influence of dot B, which is still present, must be investigated. Therefore we measured G as a function of magnetic field and top gate voltage. In contrast to side gate 1, which couples mainly to dot A, the top gate has a stronger influence on dot B. Thus we can expect to see features from both dots at once.

The measurement is shown in Fig. 3(a). Again we observe oscillating peak positions in the Coulomb peaks of dot A. But a detailed look reveals that these peaks are split by local minima in differential conductance. These minima are colored white in the highlighted section and show a pattern of more or less horizontal lines with regular distance in V_{TG} . These lines refer to transitions on dot B and correspond to the splitting of triple points in Fig. 1(b). As the Coulomb peaks of dot A are split, parts of each peak are above a splitting and others are below (dotted and solid red lines in the section). Therefore we can compare the peak amplitudes of each Coulomb peak below and above a splitting and can directly investigate the effect of capacitive dot–dot coupling on the peak amplitude. This is done in Fig. 3(b). For each peak visible in Fig. 3(a) the peak amplitude is plotted as a function of magnetic field. For all peaks both amplitudes below a splitting (solid line) and above a splitting (dotted line) fit almost perfectly together and the typical oscillations of high and low amplitude become visible. Thus the influence of capacitive interdot coupling is identified as a pure peak splitting effect without any impact on the peak amplitude. In consequence we find our assumption verified that the oscillations in peak position and amplitude ascribe to a single dot spin blockade of dot A. As a result this spin blockade is

not destroyed by capacitive interdot coupling, it is not even affected at all.

In summary we have investigated spin blockade in a tunable double dot device fabricated by LAO. We have characterized the system regarding the tunability of the interdot coupling as a function of top gate voltage and magnetic field. In the regime of capacitive coupling we observed single dot spin blockade. We have shown that this spin blockade is not destroyed or at least affected by transitions on the capacitively coupled dot. Therefore it is a very useful tool for spin detection even in LAO based quantum dot devices.

The authors thank M. Bichler, G. Abstreiter, and W. Wegscheider for the heterostructure, D. Pfannkuche for helpful discussions, and F. Hohls for careful reading of the manuscript. This work has been supported by BMBF.

- ¹L. P. Kouwenhoven, C. M. Marcus, P. L. McEuen, S. Tarucha, R. M. Westerveld, and N. S. Wingreen, in *Mesoscopic Electron Transport*, edited by L. L. Sohn, L. P. Kouwenhoven, and G. Schön (Kluwer, Dordrecht, 1997), Vol. 345 of Series E, pp. 105–214.
- ²W. G. van der Wiel, S. D. Franceschi, J. M. Elzerman, T. Fujisawa, S. Tarucha, and L. P. Kouwenhoven, *Rev. Mod. Phys.* **75**, 1 (2003).
- ³A. W. Holleitner, R. H. Blick, A. K. Hüttel, K. Eberl, and J. P. Kotthaus, *Science* **297**, 70 (2002).
- ⁴C. Livermore, C. H. Crouch, R. M. Westerveld, K. L. Campman, and A. C. Gossard, *Science* **274**, 1332 (1996).
- ⁵F. Hofmann, T. Heinzel, D. A. Wharam, J. P. Kotthaus, G. Böhm, W. Klein, G. Tränkle, and G. Weimann, *Phys. Rev. B* **51**, 13872 (1995).
- ⁶L. W. Molenkamp, K. Flensberg, and M. Kemerink, *Phys. Rev. Lett.* **75**, 4282 (1995).
- ⁷D. Loss and D. P. DiVincenzo, *Phys. Rev. A* **57**, 120 (1998).
- ⁸D. Weinmann, W. Häusler, and B. Kramer, *Phys. Rev. Lett.* **74**, 984 (1995).
- ⁹K. Ono, D. G. Austing, Y. Tokura, and S. Tarucha, *Science* **297**, 1313 (2002).
- ¹⁰M. Ciorga, A. S. Sachrajda, P. Hawrylak, C. Gould, P. Zawadzki, S. Juliano, Y. Feng, and Z. Wasilewski, *Phys. Rev. B* **61**, R16315 (2000).
- ¹¹M. Ciorga, A. Wensauer, M. Piore-Ladriere, M. Korkusinski, J. Kyriakidis, A. S. Sachrajda, and P. Hawrylak, *Phys. Rev. Lett.* **88**, 256804 (2002).
- ¹²M. Ciorga, M. Piore-Ladriere, P. Zawadzki, P. Hawrylak, and A. S. Sachrajda, *Appl. Phys. Lett.* **80**, 2177 (2002).
- ¹³M. Piore-Ladriere, M. Ciorga, J. Lapointe, P. Zawadzki, M. Korkusinski, P. Hawrylak, and A. S. Sachrajda, *Phys. Rev. Lett.* **91**, 026803 (2003).
- ¹⁴M. C. Rogge, C. Fühner, U. F. Keyser, R. J. Haug, M. Bichler, G. Abstreiter, and W. Wegscheider, *Appl. Phys. Lett.* **83**, 1163 (2003).
- ¹⁵R. H. Blick, R. J. Haug, J. Weis, D. Pfannkuche, K. v. Klitzing, and K. Eberl, *Phys. Rev. B* **53**, 7899 (1996).
- ¹⁶R. H. Blick, D. Pfannkuche, R. J. Haug, K. v. Klitzing, and K. Eberl, *Phys. Rev. Lett.* **80**, 4032 (1998).
- ¹⁷J. M. Golden and B. I. Halperin, *Phys. Rev. B* **54**, 16757 (1996).
- ¹⁸P. L. McEuen, E. B. Foxman, J. M. Kinaret, U. Meirav, M. A. Kastner, S. Wingreen, and S. J. Wind, *Phys. Rev. B* **45**, 11419 (1992).
- ¹⁹A. Fuhrer, S. Lüscher, T. Ihn, T. Heinzel, K. Ensslin, W. Wegscheider, and M. Bichler, *Phys. Rev. B* **63**, 125309 (2001).
- ²⁰R. Held, S. Lüscher, T. Heinzel, K. Ensslin, and W. Wegscheider, *Appl. Phys. Lett.* **75**, 1134 (1999).